Maximum heat transfer rate density in two-dimensional minichannels and microchannels

Michel Favre-Marinet, Stéphane Le Person, A. Bejan

MAXIMUM HEAT TRANSFER RATE DENSITY IN TWO-DIMENSIONAL MINICHANNELS AND MICROCHANNELS

M. Favre-Marinet and S. Le Person
Laboratoire des Ecoulements Géophysiques et Industriels CNRS-UJF-INPG, Grenoble Cedex, France

A. Bejan
Duke University, Department of Mechanical Engineering and Materials Science, Durham, North Carolina, USA

The objective of the present article is to compare previous experimental data of Gao et al. [20] to the predictions of Bejan and Sciubba's analysis [7] on the optimal spacing for maximum heat transfer from a package of parallel plates. Experimental investigations of the flow and the associated heat transfer were conducted in two-dimensional microchannels in order to test possible size effects on the laws of hydrodynamics and heat transfer and to infer optimal conditions of use from the measurements. The test section was designed to modify easily the channel height e between 1 mm and 0.1 mm. Measurements of the overall friction factor and local Nusselt numbers show that the classical laws of hydrodynamics and heat transfer are verified for $e > 0.4$ mm. For lower values of e, a significant decrease of the Nusselt number is observed, whereas the Poiseuille number continues to have the conventional value of laminar developed flow. The transition to turbulence is not affected by the channel size. The experimental data were processed by using the dimensionless parameters of Bejan and Sciubba's analysis [7]. For fixed pressure drop across the channel, a maximum of heat transfer rate density is found for a particular value of e. The corresponding dimensionless optimal spacing and heat transfer rate density are in very good agreement with the predictions of Bejan and Sciubba. This article reports the first time that the optimal spacing between parallel plates is determined experimentally.

Keywords microfluidics, heat transfer, microchannels, optimization

INTRODUCTION

The development of microscale systems has grown rapidly during the last decades, making possible many applications. In the field of heat transfer, use of microchannels

This research was supported by the CNRS and Region Rhône-Alpes. The authors gratefully acknowledge Institut National Polytechnique de Grenoble for supporting the visit of A. Bejan in Grenoble. They also thank P. Gao for performing the experiments.

This paper was presented at the First International Conference on Microchannels and Minichannels on April 24–25, 2003, at Rochester, New York.

Address correspondence to Michel Favre-Marinet, Laboratoire des Ecoulements Géophysiques et Industriels, CNRS-UJF-INPG, 1025 rue de la Piscine, Grenoble Cedex, BP 53 X, 38041, France. E-mail: Michel.Favre-Marinet@hmg.inpg.fr

NOMENCLATURE

b	channel width (spanwise direction), m
D_h	hydraulic diameter, m
e	channel height, m
f	Fanning friction factor, dimensionless
h	heat transfer coefficient, $W \cdot m^{-2} \cdot K^{-1}$
k	thermal conductivity, $W \cdot m^{-1} \cdot K^{-1}$
L	channel length, m
$L^+ = \frac{L}{D_h} \frac{1}{\mathrm{Re}}$	dimensionless channel length
L_h	heated channel length used in optimization analysis, m
l_h	heating resistance length, m
Nu	Nusselt number, dimensionless
P	electric power, W
p	pressure, $N \cdot m^{-2}$
Po	Poiseuille number, dimensionless
Pr	Prandtl number, dimensionless
q''	heat flux, $W \cdot m^{-2}$
$\tilde{q}''$	dimensionless heat flux,
Q	total heat transfer rate, W
Q_v	volumetric flow rate, m^3/s
$\mathrm{Re} = \frac{\rho V D_h}{\mu}$	Reynolds number, dimensionless
T	temperature, °C
V	channel bulk velocity, $m \cdot s^{-1}$
x	abscissa along the channel, m
$x^+ = \frac{x}{D_h} \frac{1}{\mathrm{Re}}$	hydrodynamic entrance parameter, dimensionless
$x^* = \frac{x}{D_h} \frac{1}{\mathrm{RePr}}$	thermal entrance parameter, dimensionless

Greek Symbols

α	thermal diffusivity, $m^2 \cdot s^{-1}$
μ	dynamic viscosity, $kg \cdot m^{-1} \cdot s^{-1}$
Π_L	pressure drop number, dimensionless
ρ	density, $m^3 \cdot s^{-1}$
τ	wall shear stress, $N \cdot m^{-2}$

Subscripts

av	average
c	critical
f	fluid
film	film
in	inlet
out	outlet
w	wall

seems very promising for cooling electronic equipment. Enhancement of heat transfer coefficient is obviously expected with reduction of length scales, and this has been observed many times, starting with the experiments of Tuckerman and Pease [1]. However, at the same time, pressure losses are rising very rapidly when the passage of the flow is strongly reduced. It is therefore important to consider the optimization of the design of microchannels for proper application to heat transfer problems. Since the work of Tuckerman and Pease [1], several investigations have been undertaken for optimizing heat transfer in micro heat sinks with the classical fin analysis method [2, 3]. Kim and Kim [4] used a different approach and the microchannel heat sink was modeled as a porous medium in their analysis. Very recently, a three-dimensional analysis procedure for the thermal performance of a microchannel heat sink has been developed and applied to optimize the heat sink design [5]. In this study, Ryu et al. assumed a fully developed flow, but took into account the development of thermal boundary layers. They obtained the optimum values of geometric parameters for particular working conditions (pumping power, overall dimensions), but did not bring out general rules for optimization design. The analysis was also applied to a new type of microchannel heat sink based on the principles of a manifold heat sink [6]. All these studies deal with plate-and-fin extended surfaces. They consider a heat sink base where the thermal boundary conditions are given and convective cooling by a flow in microchannels separated by fins.

In sum, most studies adopted the classical fin analysis method and used the assumption of fully developed flow and uniform heat exchange coefficient in the microchannels. On the other hand, Bejan and Sciubba [7] showed that the optimal spacing for maximum heat transfer from a package of parallel plates results from a competition between high

heat exchange coefficient of the boundary layer type for large plate spacing and large exchange surface in the opposite situation of small plate spacing. Bejan and Sciubba assumed that the pressure drop is fixed and showed that the optimal spacing is such that the channel length is equal to the entrance length. This analysis raises some questions about previous optimization studies, which do not take into account the development of boundary layers in the channels. To our knowledge, the present article is the first attempt to determine experimentally the optimal spacing between parallel plates and to test Bejan and Sciubba's predictions.

A second issue of this article concerns the scaling laws pertaining to the hydrodynamics and heat transfer in microchannels, which are not clearly established, although many studies have been devoted to this subject in recent years. Published experimental results question the applicability of classical laws (friction factor, laminar-turbulent transition, heat exchange coefficient) when the characteristic dimensions of the channel are of the order of several hundred to one μm. A recent review article [8] shows the dispersion of results from last decade experiments.

The following discussion is restricted to rectangular microchannels. Microchannels of this type may be obtained by micromachining in a metal substrate. Peng et al. [9] studied such microchannels of various sizes (hydraulic diameter D_h: 133–367 μm) micromachined in a stainless steel substrate. In the laminar regime, they generally found increase of the friction factor f. On the contrary, Xu et al. [10] found that characteristics of flow in microchannels (D_h: 56–260 μm) agree with conventional laws of hydrodynamics. Pfund et al. [11] investigated microchannels made in a sandwich structure with plates in organic material and observed friction factors greater than the classical values.

Microchannels may also be obtained by etching in silicon wafers. In several publications, the cross-section is trapezoidal because a wet anisotropic technique was used for etching the microchannel. However, the cross-section shape is not far from rectangular when the channel height is small compared to the mean width, and comparison can be made with studies on rectangular microchannels. Flockhart and Dhariwal [12] found no scale effects on hydraulics in such trapezoidal channels (27 or 63 μm in height, 1 mm in width, Reynolds number $<$240). On the contrary, Qu et al. [13] observed a significant increase of f in the same type of channels (height 28 to 111 μm, width 380 μm for the smallest height) in all the range of Re investigated (until 1600).

Transition to turbulence is also controversial. Peng et al. [9] observed much earliest transition ($\mathrm{Re}_c \sim 200$–700) in their smallest microchannels than in conventional channels. This trend was not observed in other studies [10, 14]. A smaller reduction in transition Reynolds number was found by Pfund et al. [11]. Some possible microscale effects were suggested by Mala et al. [15], Guo and Li [16], and Koo and Kleinstreuer [17].

Results on single-phase heat transfer are also contradictory. In the laminar regime, Peng et al. [9], Qu et al. [18] obtained data for the Nusselt number well below the values predicted by classical theory. The same trend was observed by Hegab et al. [14] in microchannels milled into an aluminium plate. On the contrary, Qu and Mudawar [19] conducted both experimental and numerical investigations and found good agreement of the measured temperature distributions with the numerical predictions based on the conventional mass, momentum, and energy equations.

All these studies refer to microchannels of moderate aspect ratio (width/height $\sim$ 3–4), and the results may be affected by the shape of cross-section, in addition to size effects. Recent investigations were conducted by Gao et al. [20, 21] in very high aspect

ratio (25–250) rectangular microchannels in order to approach a two-dimensional situation and to eliminate the cross-section shape from the possible factors likely to affect the flow and heat transfer. They measured the friction factor and the heat transfer coefficient in mini/microchannels of various heights (0.1–1 mm). Their experimental conditions and results are summarized in the next sections of the article.

The objective of the present article is to compare the experimental data from Gao et al. [20] to the predictions of Bejan and Sciubba's analysis [7] and to describe the optimal conditions for use in the design of micro heat exchangers.

EXPERIMENTAL FACILITY AND PROCEDURE

Experimental Setup

Flows of demineralized water in channels of large-span rectangular cross-section and adjustable height were investigated. Details on the facility may be found in Gao et al. [20]. In the experimental setup (Figure 1), the active channel walls are two plane bronze blocks, which are separated by a foil (thickness e) with a hollowed-out central part of width b (= 25 mm). The thickness of this foil fixes the channel height e, which can be varied in the range 0.1–1 mm by steps of 0.1 mm. The other dimensions of the channel are b and the length L (= 82 mm). The main advantage of this arrangement is that the channel walls are represented by the same surfaces and that only the channel height e is varied during all the experiments. The two blocks are rounded off in the upstream part to form a convergent channel entrance. They were hand-polished (measured roughness <0.1 μm). Two sumps are machined in the working section at the channel inlet/outlet. Heating was provided by four electric cartridges (maximum total power of 4×250 W; typical value of power used in the experiments: 200–500 W), which were inserted inside the two blocks and surrounded by an insulating material. The active length of the resistances l_h (= 62 mm) was smaller than the channel length.

Representative flow conditions are presented in Table 1. The origin of abscissa x along the channel is the beginning of the straight section.

Instrumentation

Flow rates were measured with two high-precision turbine flowmeters. The pressure drop Δp was determined by piezo resistive strain gauge transmitters (full scale: 10^6 N $\cdot$ m^{-2}) at the channel inlet/outlet, or by a differential gauge (full scale: 10^4 N $\cdot$ m^{-2}). Thermocouples of type K were placed in the two sumps to determine the fluid inlet/outlet temperatures, denoted respectively T_{in} and T_{out}. Wall temperatures were measured by five thermocouples (denoted TC_1 to TC_5) of type T (diameter = 0.5 mm) placed in 1.5 cm increments along the channel (position of the first thermocouple $x = 0.6$ cm). The corresponding sections are denoted "1" to "5." The thermocouples were located in the bronze blocks 1 mm away from the metal–fluid interface.

Data Processing

The data were interpreted by using the Reynolds number Re and the Nusselt number Nu, which were defined based on the hydraulic diameter D_h. Re was based on the

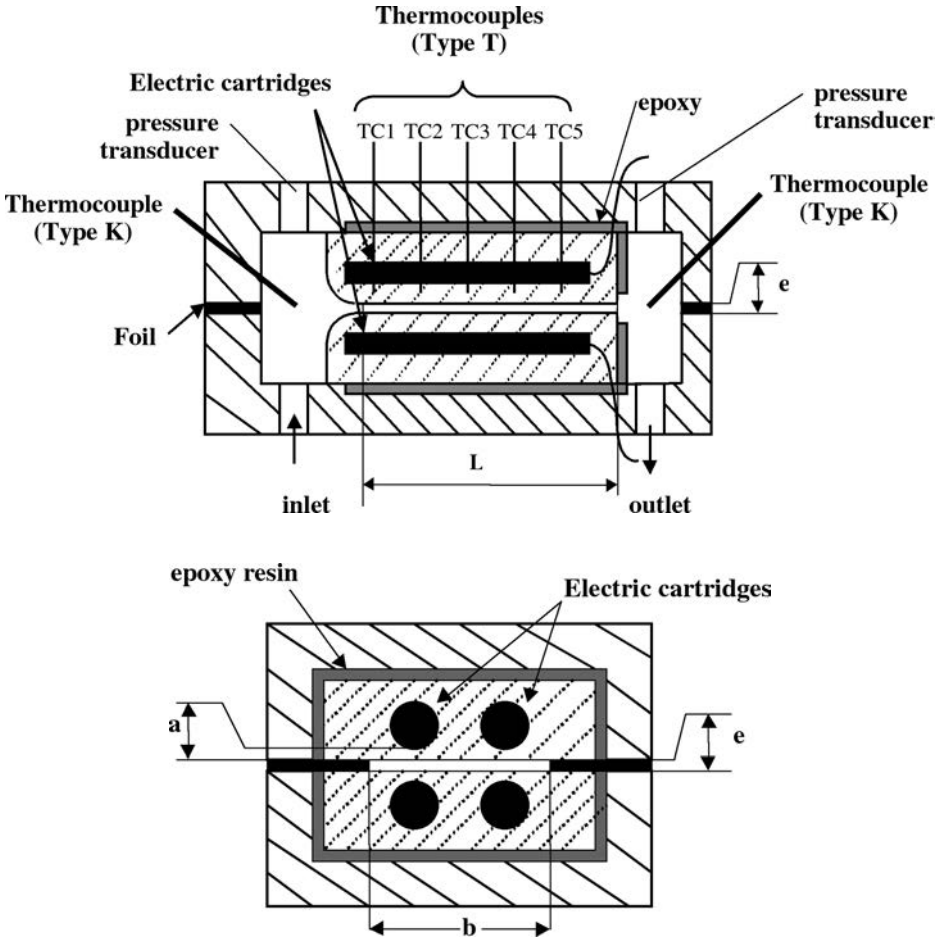

Figure 1. Sketch of the test section.

Table 1. Typical flow conditions

e	b (mm)	L (mm)	U (m/s)	Q_v (1/mn)	Re
100 μm	25	82	0.1–10	0.015–1.5	20–2400
200 μm	25	82	0.16–15	0.05–4.5	57–6000
1 mm	25	82	0.02–4	0.03–6	40–7400

bulk velocity in the channel. The water properties, such as density, dynamic viscosity, and Prandtl number, were determined at the average of the inlet/outlet temperatures T_{av} ($= [1/2][T_{\text{in}}+T_{\text{out}}]$). The thermal conductivity used in Nu was determined at the local film temperature T_{film} (average of wall and fluid bulk temperatures; $T_{\text{film}} = [1/2][T_{\text{w}} + T_{\text{f}}]$). The friction factor f was determined from the inlet/outlet pressure measurements. The

inlet pressure was corrected for the inertia term accounting for flow acceleration in the converging channel entrance. The classical hypothesis of constant pressure in the outlet sump was made to evaluate the pressure at the channel outlet. In other words, the head losses were neglected in the converging inlet channel and were concentrated at the channel outlet. The pressure drop across the microchannels was therefore estimated by:

$$\Delta p = p_{\text{in}} - p_{\text{out}} - (1/2)\rho V^2 \tag{1}$$

where p_{in} and p_{out} are measured at inlet/outlet sumps, respectively (Figure 1). The friction factor was given by:

$$f = \frac{\tau}{(1/2)\rho V^2} = \frac{\Delta p}{2\rho V^2} D_h L \tag{2}$$

The local wall heat flux q'' was deduced from the electric power P assumed uniformly distributed along the resistances. The local fluid bulk temperature was deduced from a heat balance between the heat rate exchanged with the walls and the rate of enthalpy convected by the stream. Close agreement was found for the rate of enthalpy convected by the stream across the channel and the electric power dissipated in the blocks, except for very small flow rates. In this last case, incorrect measurements of T_{out} are suspected. A one-dimensional model was developed to account for conduction in the metallic slab, which is located between the resistances and the channel. From these computations it was found that the measurements in sections 2 and 3 are not affected by conductive effects and may be used to determine the heat transfer coefficient in the channel (for more details, see Gao et al. [20]). It was also verified that the local fluid bulk temperature T_f may be assumed to vary linearly along the channel over the length l_h. The heat exchange surface was assumed to correspond to the active length of the resistances. The local Nusselt number was then computed from the measurements by using the following relations

$$q'' = \frac{P}{2bl_h} \tag{3}$$

$$T_{\text{f}} = T_{\text{in}} + (T_{\text{out}} - T_{\text{in}})\frac{x}{l_h} \tag{4}$$

$$h = \frac{q''}{T_{\text{w}} - T_{\text{f}}} \tag{5}$$

$$\text{Nu}_x = \frac{h D_h}{k} \tag{6}$$

When Q was smaller than the electric power P, Q was used instead of P in Eq. (3). Uncertainties were analyzed and estimated. The results are given in Table 2.

RESULTS

The next two sections summarize the results found by Gao et al. [20].

Table 2. Uncertainty analysis for $100 < \mathrm{Re} < 8000$

e (mm)		1 (%)	0.5 (%)	0.1 (%)
dRe/Re	Mini	0.4	0.4	0.4
	Maxi	0.8	0.7	0.7
dNu/Nu	Mini	0.6	0.7	0.4
	Maxi	7.8	4.9	1.2

Friction Factor

For low values of the Reynolds number the flow is laminar, but entrance effects are present and affect the total pressure drop across the channel. The wall boundary layers merge at a distance $x^+ \approx 0.04$ [22]. Because the length of the tested channels is fixed, the entrance length depends on the channel height and on the flow velocity. It is therefore helpful to plot the pressure drop as a function of the dimensionless channel length L^+. The Poiseuille number

$$\mathrm{Po} = f\mathrm{Re} \tag{7}$$

deduced from the measurements is drawn in Figure 2 for the lowest values of e. The graph also displays the following formula proposed by Shah [23]:

$$\mathrm{Po} = \frac{3.44}{\sqrt{L^+}} + \frac{24 + 0.674/4L^+ - 3.44/\sqrt{L^+}}{1 + 2.9 \times 10^{-5}/L^{+2}} \tag{8}$$

Figure 2 shows that the friction law for the developed laminar flow regime ($f\mathrm{Re} = 24$) is confirmed very well by the present experiment, regardless of the channel height. Equation (8) slightly overestimates the pressure drop in the range $0.1 < L^+ < 1$. A clear departure from Eq. (8) is observed when L^+ is lower than a critical value L_c^+,

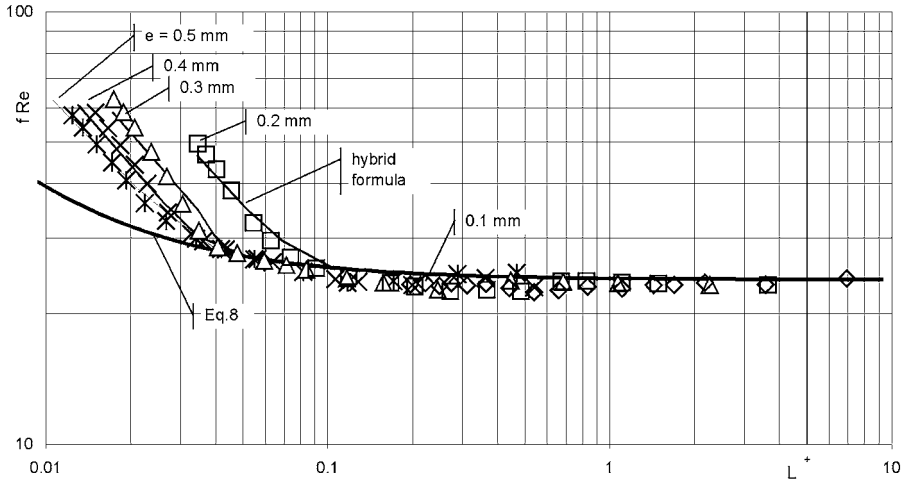

Figure 2. Effect of channel size on the nondimensional pressure drop.

which depends on the channel height. L_c^+ obviously corresponds to a critical value of the Reynolds number Re_c. It was found that Re_c does not depend significantly on e and is approximately equal to 3500, close to the accepted value of 4000 for transition in plane wall channels. This result was also confirmed by visualizations obtained by dye injection at the channel inlet. Solid lines in Figure 2 correspond to a hybrid formula using Eq. (8) in the first half of the channel and the Blasius equation

$$f = 0.079\mathrm{Re}^{-1/4} \tag{9}$$

in the second part of the channel. The good agreement with the experimental data also confirms the existence of the turbulent regime for $\mathrm{Re} > \mathrm{Re}_c$.

Heat Transfer Coefficient

For a given flow rate, four values of the local Nusselt number Nu_x were obtained from the thermocouples TC_1 to TC_4 by using Eqs. (3) to (6). As for pressure losses, the local Nusselt number Nu_x was plotted as a function of x^* ($= x/[D_h\ \mathrm{Re}\ \mathrm{Pr}]$) in order to identify entrance effects and transition to turbulence in the heat transfer results. Figure 3 shows the results for $e = 0.5$ mm and $e = 0.1$ mm. The data of Shah and London [24] for simultaneous developing flow and heat transfer were interpolated for $\mathrm{Pr} = 4$ and displayed in the same figure.

The general trend observed for all the channels tested is in good agreement with the data of Shah and London [24] for $e \geq 0.5$ mm. There is a significant decrease in Nu_x when the channel height is decreased below 0.5 mm. A satisfying overlap of the results deduced from the four thermocouples was observed, which confirms that x^* is the relevant parameter for the heat transfer results. However, for each channel height, two systematic deviations from the general trend were observed. A deviation toward low values of Nu_x and, more generally, an important scatter of the results occur when x^* is increased for a given thermocouple; that is, when the flow rate is decreased. In fact, the observed rapid decrease of Nu_x is not linked to x^*, as can be seen in Figure 3, but to

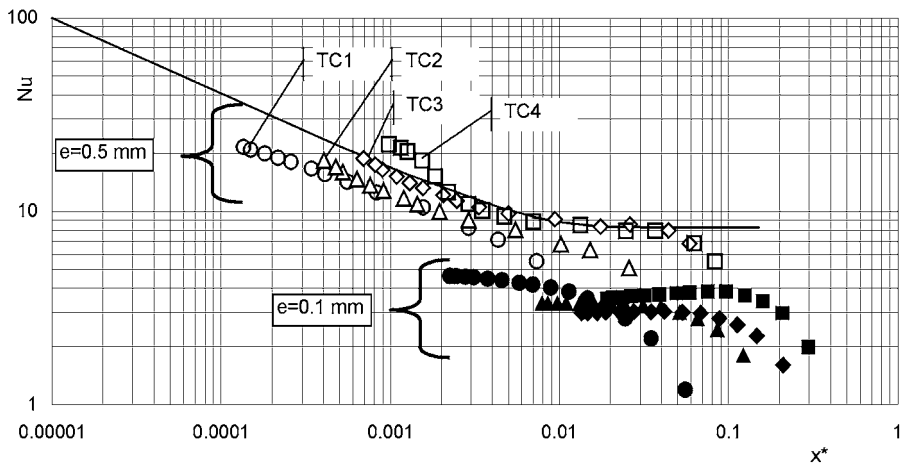

Figure 3. Local Nusselt number.

the small flow rates used in these conditions since it occurs for the same flow rate at the four measurement sections. This reduction of Nu_x corresponds to the low values of the total enthalpy rise Q measured for the smallest flow rates, as mentioned before. It is likely that Q is incorrectly determined in these conditions and that the corresponding results for Nu_x are not reliable. Consequently, they were discarded in the optimization analysis. On the other hand, the values of Nu_x given by TC_4 are significantly above the other results for small values of x^* (<0.002 for $e = 0.5$ mm in Figure 3) for all the channels. This range of x^* corresponds to TC_4 at the highest flow rates and highest Re used in the experiments. The Reynolds number found for the change of slope in the Nu_x-curve is close to the value deduced from pressure losses measurements. Consequently, this change of regime for heat transfer may be attributed to the transition to turbulence in the microchannel.

The significant decrease observed in the Nusselt number with the size of the channel is in agreement with previously published results [18]. It was also observed in experimental investigations on heat transfer with a microtube [25]. Figure 3 shows that it can reach a factor of about 30% for $e = 0.1$ mm ($Nu \approx 3$ instead of 8.23 for the fully developed laminar regime). A numerical modeling of the fluid flow and heat transfer in this experiment is now in progress [26].

Optimal Spacing of the Plates in a Micro Heat Exchanger

The optimal spacing for maximum heat transfer from a package of parallel plates was investigated both theoretically and numerically by Bejan and Sciubba [7] (see also Bejan [27]). In this study, the authors considered an arrangement of parallel plates cooled by forced convection and found a maximum heat transfer rate for fixed pressure drop and fixed inlet and wall temperatures. They also considered the case of uniform heat flux surfaces. It should be stressed that this arrangement is different from a heat sink with parallel fins, which is used in most optimization studies [1–5]. In this last case, the total heat flux is released at the heat sink surface and the thermal resistance of the structure depends on the fin efficiency, whereas the wall temperature or the heat transfer rate density are assumed uniform along the plates in Bejan and Sciubba's study. These authors showed that the relevant parameters are the dimensionless heat transfer rate density

$$\tilde{q}'' = \frac{2q''L_h^2}{e \cdot k(T_{\max} - T_{\min})} \tag{10}$$

and the pressure drop number (which earlier Bhattacharjee and Grosshandler [28] had termed the Bejan number; see also Petresen [29]):

$$\Pi_L = \frac{\Delta p_{L_h} L_h^2}{\mu\alpha} \tag{11}$$

Here Δp_{L_h} is the pressure drop over a channel of length L_h. $T_{\max}$ is the wall temperature for $x = L_h$ and $T_{\min}$ is the fluid inlet temperature. The theoretical analysis suggests that the optimal spacing for maximum heat transfer is given by

$$e/L_h = a_1 \Pi_L^{-1/4} \tag{12}$$

and that the maximum power density satisfies

$$\tilde{q}'' = a_2 \Pi_L^{1/2} \tag{13}$$

The constants a_1 and a_2 depend slightly on Pr and on the thermal boundary conditions. Bejan and Sciubba [7] found: $a_1 = 3.077$, $a_2 = 0.522$ for Pr = 6 and isothermal surfaces, and $a_1 = 3.287$, $a_2 = 0.424$ for Pr = 10 and uniform heat flux surfaces.

The present experimental data were analyzed by using this scale analysis. The actual conditions of heating were close to the case of a constant flux channel. However, the maximum temperature did not occur at the channel exit, owing to the reduced heating resistance length, as mentioned before. Section 3 of the thermocouple TC_3 ($x = L_h = 3.6$ cm) was chosen to analyze the data because it is not affected by wall conduction effects regardless of the flow conditions and may be assumed to be in a region of constant heat flux for all the channels [20]. The pressure drop between inlet and section 3 was deduced from the measured total pressure drop Δp across the channel (Eq. (1)) by using the following relation:

$$\Delta p_{\text{inlet}-\text{“3”}} = \Delta p - \Delta p_{\text{“3”}-\text{outlet}} \tag{14}$$

In most cases, section 3 was located in the fully developed region and it was possible to estimate the pressure drop $\Delta p_{\text{“3”}-\text{outlet}}$ by the classical laws of friction for fully developed flow in the laminar or the turbulent regime, depending on the value of Re (f Re = 24 for Re $<$ Re_c and Eq. (9) for Re $>$ Re_c).

When the resulting $\Delta p_{\text{inlet}-\text{“3”}}$ was less than 100 N $\cdot$ m^{-2}, the data were discarded because the resulting pressure difference corresponds to the accuracy of the differential pressure transmitter. This occurred especially for the largest channels because the pressure drop is small in this case. All the data were kept for $e = 0.1$, 0.2 mm, but 25% were eliminated for 0.3 mm $\leq e \leq$ 0.7 mm and 50% for $e = 1$ mm.

Each series of experiments was conducted at constant channel height, for obvious practical reasons, and constant heat flux. As a consequence, the pressure drop and the maximum temperature were variable during the experiments, but the data may then be processed at constant pressure drop, as in the theoretical analysis. In fact, following the results of the theoretical analysis (Eqs. (12)–(13)), the present data are plotted by using $\tilde{q}''/\Pi_L^{1/2}$ as a function of $\frac{e}{L_h}\Pi_L^{1/4}$ in Figure 4. In spite of the lack of measurements for very low values of $\frac{e}{L_h}\Pi_L^{1/4}$, the present results clearly show an optimal spacing for $\frac{e}{L_h}\Pi_L^{1/4} \approx 3$ for the narrowest microchannels investigated ($e = 0.1$–0.4 mm). The maximum values of $\tilde{q}''/\Pi_L^{1/2}$ are slightly less than predicted by the theory, but the agreement with Bejan and Sciubba's prediction is good. The curve corresponding to $e = 0.1$ mm is shifted toward lower values of $\tilde{q}''/\Pi_L^{1/2}$. This is due to the strong reduction in the Nusselt number, which was observed for these conditions (Figure 3). Very few points were obtained on the left branch of the curves of Figure 4, especially for $e > 0.5$ mm, because they correspond to a very low pressure drop across the channel and consequently to the low range of the differential pressure transmitter.

The theoretical analysis shows that the position of the $\tilde{q}''$ maximum corresponds to $x^* \approx 0.04$. Bejan and Sciubba [7] remarked that the optimal spacing is therefore such that the channel length is equal to the thermal entrance length. The present experiments

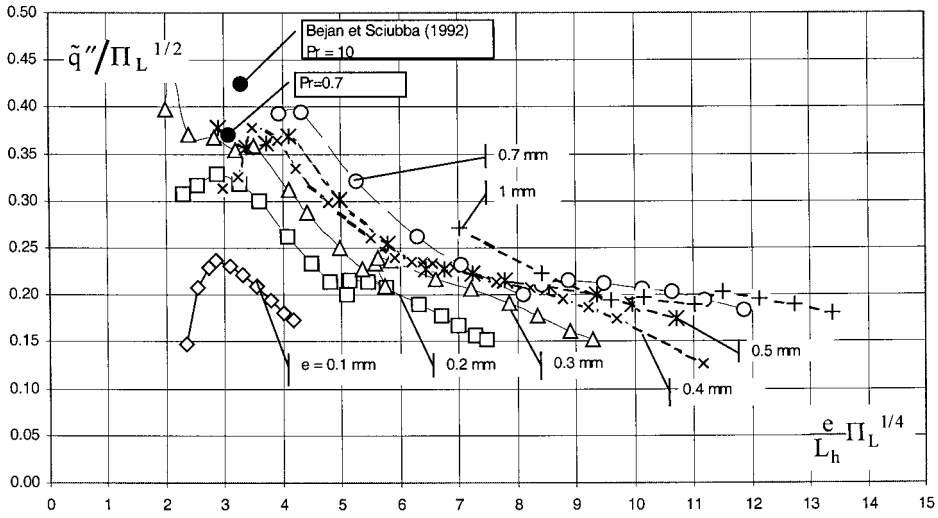

Figure 4. Optimal spacing for maximum heat transfer.

provide strong support to the theoretical prediction for $e = 0.1$ mm ($x^* = 0.046$) and for $e = 0.2$ mm ($x^* = 0.041$). The agreement deteriorates at $e = 0.4$ mm ($x^* = 0.018$), but the position of the maximum is not well defined in this case (Figure 4).

CONCLUSION

Two-dimensional microchannels were investigated in the present study. The design of the test section enabled variations of the channel height by steps of 0.1 mm, from 1 mm, which corresponds to minichannels to the smallest height of 0.1 mm, where size effects were suspected to affect the flow dynamics and heat transfer. Flow and heat transfer measurements were first interpreted by using a dimensionless distance to the channel inlet (respectively, L^+ or $x^* = x/[D_h \text{ Re Pr}]$). This presentation clearly identifies entrance effects and transition to turbulence. The results show that the classical laws of friction in two-dimensional ducts are well verified both in the laminar and the turbulent regimes. In fact, no scale effects were found in the present experiments for the flow hydrodynamics. Heat transfer laws are also well verified for the minichannels of the present study in the laminar regime ($e \geq 0.5$ mm). However, for $e < 0.5$ mm, the plots of Nu_x (x^*) show a departure from the classical heat transfer law, which grows when the channel height is decreased. The reduction of Nu is very strong for the narrowest microchannels. For $e = 0.1$ mm, Nu is roughly 60% smaller than the conventional value for large-scale channels.

The objectives of the study were the optimization of two-dimensional channels and to test the theoretical and numerical results of Bejan and Sciubba [7]. For this purpose, the experimental data were interpreted by using the dimensionless parameters first introduced by these authors. Although the range of the dimensionless spacing $\frac{e}{L_h}\Pi_L^{1/4}$ is rather limited in the present study, especially for small spacings, an optimal spacing is clearly identified when the dimensionless heat flux $\tilde{q}''/\Pi_L^{1/2}$ and spacing $\frac{e}{L_h}\Pi_L^{1/4}$ are

used to interpret the data. The present experiments support well the predictions of Bejan and Sciubba [7], except the smaller values of maximum heat transfer rate density, which may be attributed to microscale effects. This is the first time that the optimal spacing between parallel plates was determined experimentally.

Further experiments will be conducted with other surface finishes in order to identify the phenomena governing this flow. In particular, it is planned to carry out investigations of microchannel flows with rough walls. Further insight in the flow phenomena should be provided by visualizations, which will be soon performed in a test section with transparent walls. Measurements with microsensors are also planned in the near future.

REFERENCES

1. D. B. Tuckerman and R. F. Pease, High-Performance Heat Sinking for VLSI, *IEEE Electron Device Letters*, vol. 2, no. 5, pp. 126–129, 1981.
2. V. K. Samalam, Convective Heat Transfer in Microchannels, *Journal of Electronic Materials*, vol. 18, pp. 611–617, 1989.
3. R. W. Knight, J. S. Goodling, and D. J. Hall, Optimal Thermal Design of Forced Convection Heat Sinks—Analytical, *Journal of Electronic Packaging*, vol. 113, pp. 313–321, 1991.
4. S. J. Kim and D. Kim, Forced Convection in Microstructures for Electronic Cooling, *Journal of Heat Transfer*, vol. 121, pp. 639–645, 1999.
5. J. H. Ryu, D. H. Choi, and S. J. Kim, Numerical Optimization of the Thermal Performance of a Microchannel Heat Sink, *International Journal of Heat and Mass Transfer*, vol. 45, no. 13, pp. 2823–2827, 2002.
6. J. H. Ryu, D. H. Choi, and S. J. Kim, Three-Dimensional Numerical Optimization of a Manifold Microchannel Heat Sink, *International Journal of Heat and Mass Transfer*, vol. 46, no. 9, pp. 1563–1562, 2003.
7. A. Bejan and E. Sciubba, The Optimal Spacing of Parallel Plates Cooled by Forced Convection, *International Journal of Heat and Mass Transfer*, vol. 35, pp. 3259–3264, 1992.
8. C. B. Sobhan and S. V. Garimella, A comparative Analysis of Studies on Heat Transfer and Fluid Flow in Microchannels, Microscale Thermophysical Engineering, vol. 5, pp. 293–311, 2001.
9. X. F. Peng, G. P. Peterson, and B. X. Wang, Heat Transfer Characteristics of Water Flowing Through Microchannels, *Experimental Heat Transfer*, vol. 7, pp. 265–283, 1994.
10. B. Xu, K. T. Ooi, N. T. Wong, and W. K. Choi, Experimental Investigation of Flow Friction in Microchannels, *International Communications in Heat and Mass Transfer*, vol. 27, pp. 1165–1176, 2000.
11. D. Pfund, D. Rector, A. Shekarriz, A. Popescu, and J. Welty, Pressure Drop Measurements in a Microchannel, *AIChE Journal*, vol. 46, no. 8, pp. 1496–1507, 2000.
12. S. M. Flockhart and R. S. Dhariwal, Experimental and Numerical Investigation into the Flow Characteristics of Channels Etched in ⟨ 100 ⟩ Silicon, *Journal of Fluids Engineering*, vol. 120, pp. 291–295, 1998.
13. W. Qu, G. M. Mala, and D. Li, Pressure-Driven Water Flows in Trapezoidal Silicon Microchannels, *International Journal of Heat and Mass Transfer*, vol. 43, pp. 353–364, 2000.
14. H. E. Hegab, A. Bari, and T. Ameel, Friction and Convection Studies of R-134a in Microchannels within the Transition and Turbulent Flow Regimes, *Experimental Heat Transfer*, vol. 15, pp. 245–259, 2002.
15. M. G. Mala, D. Li, and J. D. Dale, Heat Transfer and Fluid Flow in Microchannels, *International Journal of Heat and Mass Transfer*, vol. 40, no. 13, pp. 3079–3088, 1997.
16. Z. Y. Guo and Z. X. Li, Size Effect on Microscale Single-Phase Flow and Heat Transfer, *Proc. 12th International Heat Transfer Conference*, vol. 1, pp. 15–27, 2002.

17. J. Koo and C. Kleinstreuer, Liquid Flow in Microchannels: Experimental Observations and Computational Analyses of Microfluidics Effects, *Journal of Micromechanics Microengineering*, vol. 13, pp. 568–579, 2003.
18. W. Qu, G. M. Mala, and D. Li, Heat Transfer for Water Flows in Trapezoidal Silicon Microchannels, *International Journal of Heat and Mass Transfer*, vol. 43, pp. 3925–3936, 2000.
19. W. Qu, and I. Mudawar, Experimental and Numerical Study of Pressure Drop and Heat Transfer in a Single-Phase Micro-Channel Heat Sink, *International Journal of Heat and Mass Transfer*, vol. 45, pp. 2549–2565, 2002.
20. P. Gao, S. Le Person, and M. Favre-Marinet, Scale Effects on Hydrodynamics and Heat Transfer in Two-Dimensional Mini and Microchannels, *International Journal of Thermal Sciences*, vol. 41, pp. 1017–1027, 2002.
21. P. Gao, S. Le Person, and M. Favre-Marinet, Hydrodynamics and Heat Transfer in Two-Dimensional Microchannels, *Proc. 12th International Heat Transfer Conference*, vol. 2, pp. 183–188, 2002.
22. F. M. White, *Viscous Fluid Flow*, Second Edition, McGraw-Hill, New York, 1991.
23. R. K. Shah, A Correlation for Laminar Hydrodynamic Entry Length Solutions for Circular and Noncircular Ducts, *Journal of Fluids Engineering*, vol. 100, pp. 177–179, 1978.
24. R. K. Shah and A. L. London, Laminar Flow Forced Convection in Ducts, A Source Book for Compact Heat Exchanger Analytical Data, Supplement 1, in *Advanced Heat Transfer*, Academic Press, New York, 1978.
25. G. P. Celata, M. Cumo, M. Guglielmi, and G. Zummo, Experimental Investigation of Hydraulic and Single-Phase Heat Transfer in 0.130-mm Capillary Tube, *Microscale Thermophysical Engineering*, vol. 6, pp. 85–97, 2002.
26. G. Gamrat, Numerical Modelling of Heat Transfer in Microchannels, M.Sc. Thesis, University of Czestochowa, Poland, 2003.
27. A. Bejan, *Shape and Structure, from Engineering to Nature*, Chapter 3, Cambridge University Press, Cambridge, UK, 2000.
28. S. Bhattacharjee and W. L. Grosshandler, The Formation of a Wall Jet Near a High Temperature Wall Under Microgravity, *25th National Heat Transfer Conference, ASME Heat Transfer Division, Houston, Texas*, vol. 96, pp. 711–716, 1988.
29. S. Petresen, Comments on the Optimal Spacing of Parallel Plates Cooled by Forced Convection, *International Journal of Heat and Mass Transfer*, vol. 37, p. 1283, 1994.